Radiology

ORIGINAL RESEARCH • GASTROINTESTINAL IMAGING

Sex Differences and Tumor Blood Flow from Dynamic Susceptibility Contrast MRI Are Associated with Treatment Response after Chemoradiation and Long-term Survival in Rectal Cancer

Kine M. Bakke, PhD • Sebastian Meltzer, MD, PhD • Endre Grøvik, PhD • Anne Negård, MD, PhD • Stein H. Holmedal, MD • Kjell-Inge Gjesdal, PhD • Atle Bjørnerud, PhD • Anne H. Ree, MD, PhD • Kathrine R. Redalen, PhD

From the Department of Oncology, Akershus University Hospital, Epigen, Akershus Universitetssykehus HF, 1478 Lørenskog, Norway (K.M.B., S.M., K.I.G., A.H.R., K.R.R.); Department of Physics (K.M.B., A.B.) and Institute of Clinical Medicine (A.N., A.H.R.), University of Oslo, Oslo, Norway; Department of Diagnostic Physics, Division of Radiology and Nuclear Medicine, Oslo University Hospital, Oslo, Norway (E.G., A.B.); Department of Optometry, Radiography and Lighting Design, University of South-Eastern Norway, Drammen, Norway (E.G.); Department of Radiology, Akershus University Hospital, Lørenskog, Norway (A.N., S.H.H.); Sunnmøre MR-Klinikk, Ålesund, Norway (K.I.G.); and Department of Physics, Norwegian University of Science and Technology, Trondheim, Norway (K.R.R.). Received February 6, 2020; revision requested April 1; revision received July 8; accepted July 13. **Address correspondence to** K.M.B. (e-mail: *k.m.bakke@medisin.uio.no*).

Supported by the South-Eastern Norway Regional Health Authority (grant no. 2014012, 2015048, 2016050), Akershus University Hospital (grant no. 267940, 268938) and The Olav Raagholt and Gerd Meidel Raagholt Research Foundation.

Conflicts of interest are listed at the end of this article.

Radiology 2020; 00:1–9 • https://doi.org/10.1148/radiol.2020200287 • Content code: GI

Background: MRI is the standard tool for rectal cancer staging. However, more precise diagnostic tests that can assess biologic tumor features decisive for treatment outcome are necessary. Tumor perfusion and hypoxia are two important features; however, no reference methods that measure these exist in clinical use.

Purpose: To assess the potential predictive and prognostic value of MRI-assessed rectal cancer perfusion, as a surrogate measure of hypoxia, for local treatment response and survival.

Materials and Methods: In this prospective observational cohort study, 94 study participants were enrolled from October 2013 to December 2017 (ClinicalTrials.gov: NCT01816607). Participants had histologically confirmed rectal cancer and underwent routine diagnostic MRI, an extended diffusion-weighted sequence, and a multiecho dynamic contrast agent–based sequence. Predictive and prognostic values of dynamic contrast-enhanced, dynamic susceptibility contrast (DSC), and intravoxel incoherent motion MRI were investigated with response to neoadjuvant treatment, progression-free survival, and overall survival as end points. Secondary objectives investigated potential sex differences in MRI parameters and relationship with lymph node stage. Statistical methods used were Cox regression, Student *t* test, and Mann-Whitney *U* test.

Results: A total of 94 study participants (mean age, 64 years ± 11 [standard deviation]; 61 men) were evaluated. Baseline tumor blood flow from DSC MRI was lower in patients who had poor local tumor response to neoadjuvant treatment (96 mL/min/100 g ± 33 for ypT2–4, 120 mL/min/100 g ± 21 for ypT0–1; $P = .01$), shorter progression-free survival (hazard ratio = 0.97; 95% confidence interval: 0.96, 0.98; $P < .001$), and shorter overall survival (hazard ratio = 0.98; 95% confidence interval: 0.98, 0.99; $P < .001$). Women had higher blood flow (125 mL/min/100 g ± 27) than men (74 mL/min/100 g ± 26, $P < .001$) at stage 4. Volume transfer constant and plasma volume from dynamic contrast-enhanced MRI as well as ΔR_2^* peak and area under the curve for 30 and 60 seconds from DSC MRI were associated with local malignant lymph nodes (pN status). Median area under the curve for 30 seconds was 0.09 arbitrary units (au) ± 0.03 for pN1–2 and 0.19 au ± 0.12 for pN0 ($P = .001$).

Conclusion: Low tumor blood flow from dynamic susceptibility contrast MRI was associated with poor treatment response in study participants with rectal cancer.

Online supplemental material is available for this article.

In 2018, rectal cancer was the eighth most common cancer in the world (1). Survival rates have increased in the past decade mainly because of total mesorectal excision surgery and neoadjuvant treatment, when indicated. However, patients with metastatic disease remain a challenge. Norwegian patients with metastatic rectal cancer have a 5-year survival rate of 18.3% for men and 20.6% for women (2). To enable a more adapted treatment, there is a need to assess individual tumor characteristics that can be used to identify patients who will respond poorly to conventional therapies and have higher risk of metastatic disease.

Anatomic MRI is important for staging rectal cancer. Many studies have also examined the predictive and prognostic value of functional MRI, especially dynamic contrast-enhanced (DCE) MRI that can be analyzed qualitatively, semiquantitatively, or quantitatively. Recently, Dijkhoff et al (3) demonstrated value for DCE MRI in rectal cancer, despite large variability in the performed studies, and called for larger studies to be undertaken.

Abbreviations

AUC = area under the curve, BF = blood flow, DCE = dynamic contrast enhanced, DSC = dynamic susceptibility contrast, DW = diffusion weighted, HR = hazard ratio, OS = overall survival, PFS = progression-free survival

Summary

Sex differences, tumor vascularity, and blood flow seen on multiecho dynamic contrast–based MRI scans enabled prediction of treatment response and overall survival in patients with rectal cancer.

Key Results

- Dynamic susceptibility contrast MRI-assessed low tumor blood flow at baseline predicted shorter progression-free survival (hazard ratio = 0.97) and overall survival (hazard ratio = 0.98, both $P <$ .001) at median follow-up of 42 months (range, 25–71 months).
- Tumor blood flow at baseline was lower in patients who had poor local tumor response to neoadjuvant treatment (mean, 96 mL/min/100 g ± 33 [standard deviation] for ypT2–4 vs 120 mL/min/100 g ± 21 for ypT0–1; P = .01).

T1-weighted DCE MRI has been the most frequently used functional imaging method in cancers outside the brain. An alternative approach, dynamic susceptibility contrast (DSC) MRI, exploits the T2* effect of the contrast agent. DSC MRI has been mainly used to image the brain, where the blood-brain barrier keeps the contrast agent confined to the intravascular space. There has also been growing interest in an approach without a contrast agent, intravoxel incoherent motion MRI, which uses diffusion-weighted (DW) MRI to capture the microcirculation of blood in the capillary network, reflecting both diffusion and perfusion in the tumoral tissue (4).

The objective for measuring perfusion-related parameters can be attributed to the negative impact of tumor hypoxia on prognosis and therapy response. Hypoxic tumors provide insufficient oxygen supply to the cells as the result of low perfusion or low-oxygen transport to tissue. Hypoxia is a key risk indicator of tumor resistance to chemotherapy and radiation therapy (5), metastatic spread, and poor survival (6), but, to our knowledge, no reference methods for measuring tumor features related to hypoxia exist in clinical practice.

We hypothesized that functional MRI captures rectal cancer patients' individual biologic tumor features decisive for treatment outcome by quantitatively measuring MRI parameters related to tumor blood perfusion, which may serve as a surrogate measure of hypoxia. Hence, we aimed to assess predictive and prognostic value of quantitative DCE, DSC, and intravoxel incoherent motion MRI parameters with neoadjuvant treatment response, progression-free survival (PFS), and overall survival (OS) as end points. Secondary objectives investigated potential sex differences in MRI parameters and relationships with lymph node staging.

Materials and Methods

This study was performed in accordance with the Helsinki Declaration, and written informed consent was obtained from all participants. Approval was obtained from the institutional review board and the Regional Committee for Medical and Health Research Ethics.

Study Participants

Our prospective observational study (full study protocol at ClinicalTrials.gov: NCT01816607) enrolled 192 participants with suspected rectal cancer between October 2013 and December 2017 at Akershus University Hospital. Eligible participants had histologically confirmed rectal adenocarcinoma, were older than 18 years, and had no prior rectal cancer treatment. Participants were enrolled consecutively. Routine and study-specific MRI sequences were performed at baseline before treatment. Patient selection for neoadjuvant treatment was determined by the multidisciplinary team by applying the 2013 ESMO Clinical Practice Guidelines (7) and according to certain imaging findings specified in the updated 2017 version (8). For participants receiving neoadjuvant treatment, routine MRI was repeated after completed treatment. After surgery, histopathologic response to neoadjuvant therapy was scored by a specialist bowel cancer pathologist with more than 10 years of experience, applying the standard ypTN (7th edition) restaging system of primary tumor extension within or beyond the bowel wall (T stage) and the extent of regional lymph node involvement (N stage); yp indicates that participants had received

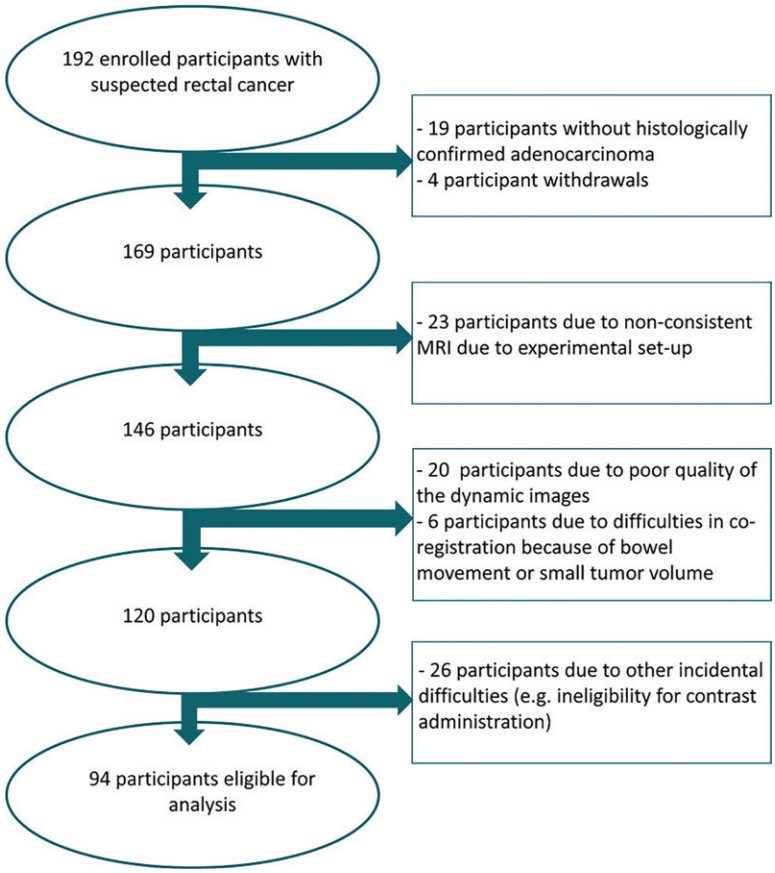

Figure 1: Flowchart of the number of participants eligible for analysis.

neoadjuvant treatment. Distant metastasis (M stage) was detected with pelvic, thoracic, or abdominal CT according to clinical practice. Data from some study participants have been previously published; 17 were in a pilot study of the multiecho MRI method (9), and 94 were in a methodologic study comparing DW, DSC, and DCE MRI (10).

MRI Examination

MRI was performed on a Philips Achieva 1.5-T system (Philips Healthcare, Best, the Netherlands). In addition to MRI for staging, the participants underwent both a dynamic multiecho MRI with an exogenous contrast agent (9,11) and an extended DW sequence. Details of the MRI sequences are found in Appendix E1 (online).

Image Postprocessing

Details of the postprocessing have been published previously (10). In brief, acquired multiecho data were used to extract two dynamic time series: T1- and T2*-weighted series. The T1-weighted signal was fitted to an extended Tofts model (12) for estimation of the volume transfer constant (K^{trans}), the rate constant (k_{ep}), the plasma volume (v_p), and the extravascular extracellular volume (v_e). The T2*-weighted signal was used in a model-free approach (13) for estimation of the perfusion-related parameter, (relative) blood flow (BF), and area under the curve (AUC) for both 30 (AUC_{30}) and 60 seconds (AUC_{60}) in addition to a measure of the ΔR_2^* (1/T2*) peak value. Analyses of the dynamic data were done in NordicICE, version 4.0 (NordicNeuroLab, Bergen, Norway).

Intravoxel incoherent motion analysis of DW data was performed by fitting the DW signal to a biexponential equation for estimation of the perfusion fraction, *f*, pseudo diffusion, *D**, and diffusion constant, *D*, using MATLAB (Mathworks, Natick, Mass).

Tumor Delineation

Tumor delineation was done independently by two radiologists (A.N., 14 years of experience; S.H.H., 7 years of experience) with experience in abdominal MRI on axial T2-weighted images with DW images serving as extra guidance and semiautomatically coregistered to the other image sequences for optimal fit. The whole tumor volume was delineated consecutively after image acquisition, and readers were blinded to clinical data. Median parameter values were extracted from the whole tumor.

Table 1: Study Participant Characteristics

Parameter	Value
No. of participants	94
No. of women	33 (35)
No. of men	61 (65)
Age (y)	64 ± 11
AJCC Stage	
1	14 (15)
Women	6 (18)*
Men	8 (13)*
2	22 (23)
Women	4 (12)*
Men	18 (30)*
3	35 (37)
Women	11 (33)*
Men	24 (39)*
4	23 (25)
Women	12 (36)*
Men	11 (18)*
TNM	
T2/T3/T4	14/46/34 (15/49/36)
N0/N1/N2	39/33/22 (42/35/23)
M0/M1	71/23 (76/24)
Treatment	
Surgery alone	49 (52)
Neoadjuvant treatment	45 (48)
Radiation 2 Gy × 25 with concomitant chemotherapy	32 (71)†
Radiation 2 Gy × 25	1 (2)†
Radiation 5 Gy × 5 and sequential chemotherapy	7 (16)†
Radiation 5 Gy × 5	4 (9)†
Only chemotherapy	1 (2)†
Survival	
PFS events‡	23 (32)
Women	5 (24)*
Men	18 (36)*
OS events	32 (34)
Women	11 (33)*
Men	21 (34)*
Main MRI parameters	
BF (mL/min/100 g)	108 ± 37
ΔR_2^*peak (au)	33.5 ± 11.8
K^{trans} (min^{-1})	0.042 ± 0.014
D^*(10^{-3} mm^2/sec)	12.1 ± 2.3

Note.—The TNM used is the seventh edition. Unless otherwise indicated, data are number of patients, with percentages in parentheses, or mean ± standard deviation. Pseudodiffusion coefficient (*D**) value is expressed as median and interquartile range. ΔR_2^*peak = maximum value of the R_2^* curve relative to the precontrast value, AJCC = American Joint Committee on Cancer, BF = blood flow, K^{trans} = volume transfer constant, OS = overall survival, PFS = progression free survival, TNM = tumor node metastasis.

* Data in parentheses are percentages of the female or male population.

† Data in parentheses are percentages of participants undergoing neoadjuvant treatment.

‡ PFS analysis were performed on the 71 stage 1–3 tumors; PFS was defined as time to local recurrence (*n* = 2), distant organ metastasis (*n* = 14), or death (*n* = 7).

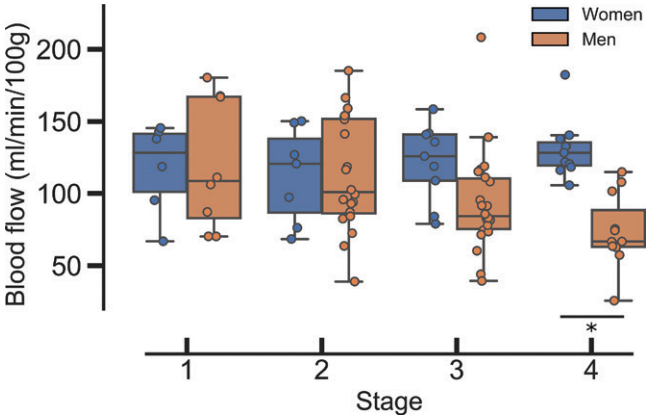

Figure 2: Tumor blood flow for the different disease stages, stratified by sex. * = statistical significance, $P < .001$.

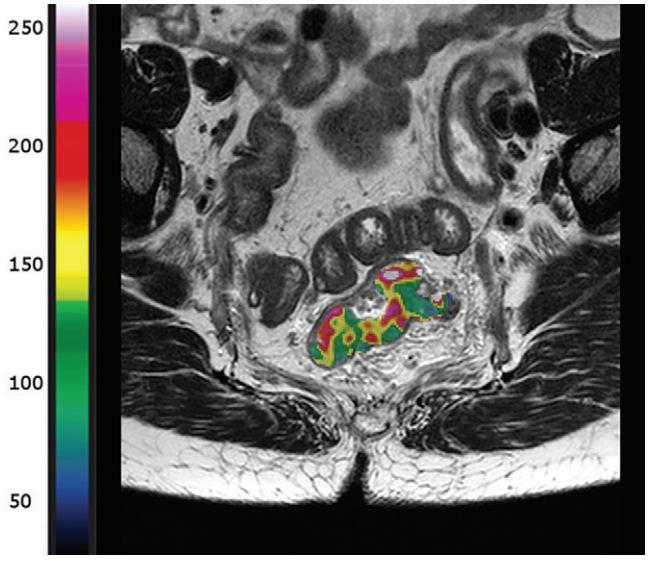

Figure 3: A 64-year-old woman with stage 4 rectal cancer (T3N2M1) with a median tumor blood flow of 140 mL/min/100 g. Image shows calculated tumor blood flow overlaid on an axial T2-weighted anatomic MRI scan. The participant had no disease progression at last follow-up. Color values are indicated on the color bar.

Serologic Factors

Lactate dehydrogenase, carcinoembryonic antigen, and C-reactive protein values were obtained from routine clinical blood sampling at baseline. Vascular endothelial growth factor A was measured with a multiplex immunoassay (Luminex; R&D Systems, Minneapolis, Minn) in serum biobank samples collected at study inclusion.

Statistical Analysis

Consistency in tumor delineation for the two radiologists was evaluated with intraclass correlation tests for all MRI-derived parameters. For differences between groups, we used the Student *t* test when data were normally distributed and a Mann-Whitney *U* test for parameters that were not, according to the Shapiro-Wilk test. To conform with the Sex and Gender Equity in Research guidelines (14), potential differences in MRI parameters with sex were evaluated in all analyses. For survival

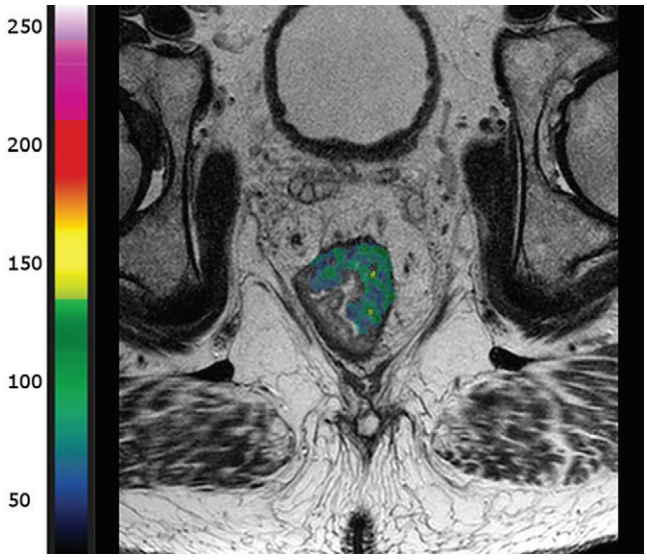

Figure 4: A 59-year-old man with stage 4 rectal cancer (T4N2M1) and a median tumor blood flow of 63 mL/min/100 g. Image shows calculated tumor blood flow overlaid on an axial T2-weighted anatomic MRI scan. The participant died after 40 months. Color values are indicated on the color bar.

analysis, we used univariable Cox regression analysis wherein sex, stage, and ypT and ypN were categorical variables and BF and D^* were continuous variables. We also did a multivariable Cox regression analysis with the significant prognostic factors from the univariable analysis. PFS was calculated from time of study enrollment to local relapse, metastatic disease, death, or final censoring for the participants without synchronous metastasis at time of diagnosis. OS was calculated from time of study enrollment to time of death or final censoring. Median follow-up for participants was 41 months (range, 25–71 months) when data were last censored on January 2, 2020. No participants were lost to follow-up. Differences in survival were visualized with Kaplan-Meier plots, in which optimal cutoffs were found by examining receiver operating characteristics curves for optimal sensitivity and specificity. Results were deemed significant at $P < .05$. All statistical procedures were performed with SPSS, version 25 (IBM, Armonk, NY).

Results

Participant Characteristics

Of the 192 participants enrolled in this study, 19 did not have histologically confirmed adenocarcinoma of the rectum, whereas four withdrew from the study (Fig 1). Because of the set-up of the experimental MRI, 23 participants had inconsistent MRI scans and were excluded. Twenty participants were excluded because of the poor quality of the dynamic images, and another six had difficulties in coregistration because of bowel movement or small tumor volumes (<5 cm^3). Other incidental difficulties led to the exclusion of another 26 participants (eg, ineligibility for contrast material administration, software updates disarranging the timing of contrast material administration). In total, 94 participants were available for analysis in this study, the demographics of which are given in

Table 1. In brief, the mean age was 64 years ± 11 [standard deviation], with 35% women and 65% men. American Joint Committee on Cancer stages 1–4 were distributed as 15%, 23%, 37%, and 25%, respectively. Fifty-two percent of the patients were scheduled for surgery alone, whereas 48% underwent neoadjuvant treatment (Table 1).

Intraclass Correlation

The intraclass correlation tests showed high correlation between observers (>0.95) for all except one parameter (Table E1 [online]); therefore, only one set of results from the two observers (A.N.) is reported.

Initial Staging

There were no overall relationships between MRI-derived parameters and tumor stage (American Joint Committee on Cancer). However, there was a difference in tumor BF for men and women in the higher tumor stages, especially for stage 4 disease (23 patients: 12 women, 11 men; 125 mL/min/100 g ± 27 for women vs 74 mL/min/100 g ± 26 for men; $P < .001$) (Fig 2). This difference was not due to age, body mass index, tumor volume, or tumor distance from the anal verge (Table E2 [online]).

Figures 3 and 4 show representative T2-weighted images with tumor BF as an overlay. Serologic factors stratified by stage and sex are summarized in Table E3 (online) and Figure E1 (online). In brief, C-reactive protein and carcinoembryonic antigen levels were higher in participants with stage 4 disease (17.0 mg/L ± 19.7 and 17.0 μg/L ± 35.5) compared with participants with localized disease (8.5 mg/L ± 15.1 and 3.0 μg/L ± 2.0, $P = .04$ and $P < .001$, respectively), probably reflecting systemic inflammation and higher tumor burden after disease dissemination. In addition, men with stage 4 disease had higher lactate dehydrogenase and carcinoembryonic antigen levels (264 U/L ± 114 and 38 μg/L ± 18.8) than women (165 U/L ± 31 and 6.3 μg/L ± 6.5, $P = .049$ and $P = .008$,

Table 2: Baseline MRI Parameters Associated with Histopathologically Determined *N*-Status (pN) in Participants with Localized Disease Scheduled for Surgery Only

Sequence and Parameter	pN0 (n = 23)	pN1–2 (n = 17)	P Value
DCE MRI			
K^{trans} (min^{-1})	0.045 ± 0.013	0.037 ± 0.010	.045*
k_{ep} (min^{-1})†	0.23 ± 0.16	0.25 ± 0.20	.94
v_p (%)†	0.14 ± 0.07	0.09 ± 0.04	.008*
v_e (%)†	10.6 ± 4.6	14.4 ± 7.4	.59
DSC MRI			
BF (mL/min/100 g)	128 ± 34	110 ± 41	.14
ΔR_2*-peak (au)	42.2 ± 10.8	30.4 ± 11.4	.002*
AUC_{30} (au)†	0.19 ± 0.12	0.09 ± 0.03	.001*
AUC_{60} (au)†	0.84 ± 0.30	0.43 ± 0.23	.004*
IVIM MRI			
f(%)	34.2 ± 5.2	35.1 ± 6.8	.44
D^* (10^{-3} mm^2/sec)†	12.6 ± 2.5	11.5 ± 5.7	.79
D (10^{-3} mm^2/sec)	0.58 ± 0.12	0.57 ± 0.12	.68

Note.—ΔR_2*peak = maximum value of the R_2* curve relative to the precontrast value, AUC_{30} = area under the curve for 30 seconds, AUC_{60} = area under the curve for 60 seconds, BF = blood flow, D = diffusion coefficient, D^* = pseudodiffusion coefficient, DCE = dynamic contrast enhanced, DSC = dynamic susceptibility contrast, f = perfusion fraction, IVIM = intravoxel incoherent motion, k_{ep} = reflux constant, K^{trans} = volume transfer constant, v_e = extracellular, extravascular volume, v_p = plasma volume.

* P value indicates a significant difference.

† Data are median and interquartile range, Mann-Whitney U test.

Table 3: Baseline MRI Parameters Associated with ypT Status in Participants Undergoing Neoadjuvant Treatment

Sequence and Parameter	ypT0–1 (n = 9)	ypT2–4 (n = 34)	P Value
DCE MRI			
K^{trans} (min^{-1})	0.047 ± 0.013	0.043 ± 0.014	.44
k_{ep} (min^{-1})*	0.20 ± 0.15	0.33 ± 0.14	.09
v_p (%)*	0.18 ± 0.07	0.10 ± 0.05	.05
v_e (%)*	14.6 ± 14.3	10.2 ± 8.1	.07
DSC MRI			
BF (mL/min/100 g)	120 ± 21	96 ± 33	.01†
ΔR_2*peak (au)	28.6 ± 10.6	30.6 ± 9.8	.59
AUC_{30} (au)*	0.10 ± 0.26	0.12 ± 0.07	.35
AUC_{60} (au)*	0.81 ± 0.62	0.51 ± 0.22	.30
IVIM MRI			
f(%)	36.0 ± 5.2	33.9 ± 5.6	.30
D^* (10^{-3} mm^2/sec)*	10.6 ± 1.5	12.3 ± 2.0	.69
D (10^{-3} mm^2/sec)*	0.58 ± 0.23	0.61 ± 0.14	.66

Note.—AUC_{30} = area under curve for 30 seconds, AUC_{60} = area under curve for 60 seconds, BF = blood flow, ΔR_2*peak = maximum value of the R_2* curve relative to the precontrast value, D = diffusion coefficient, D^* = pseudodiffusion coefficient, DCE = dynamic contrast enhanced, DSC = dynamic susceptibility contrast, f = perfusion fraction, IVIM = intravoxel incoherent motion, k_{ep} = reflux constant, K^{trans} = volume transfer constant, v_e = extracellular, extravascular volume, v_p = plasma volume.

* Median and interquartile range, Mann-Whitney U test.

† P value indicates a significant difference.

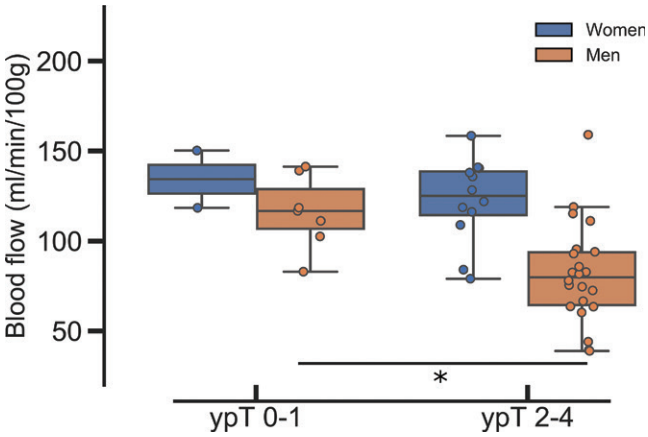

Figure 5: Tumor blood flow in participants receiving neoadjuvant treatment, stratified by local treatment response and sex. Measurements were obtained at baseline (pretreatment). * = statistical significance, $P = .006$.

respectively). In contrast, vascular endothelial growth factor A was higher in women with localized disease (1.29 pg/mL ± 0.67 for women vs 0.86 pg/mL ± 0.38 for men, $P = .02$).

Lymph Node Status

For the participants scheduled for surgery only, participants without pelvic lymph node dissemination (pN0) had higher K^{trans} (0.045 min^{-1} ± 0.013 vs 0.037 min^{-1} ± 0.010, $P = .045$), v_p (0.14% ± 0.07 vs 0.09% ± 0.04, $P = .008$), ΔR_2^* peak (42.2 ± 10.8 vs 30.4 ± 11.4, $P = .002$), AUC_{30} (0.19 ± 0.12 vs 0.09 ± 0.03, $P = .001$), and AUC_{60} (0.84 ± 0.30 vs 0.43 ± 0.23, $P = .004$) values than participants with lymph node involvement (pN1–2) (Table 2). There were no significant associations with serologic factors (Table E4 [online]).

Treatment Response in Participants Scheduled for Neoadjuvant Treatment

For the group in its entirety, tumor BF was higher in good responders (120 mL/min/100 g ± 21 for ypT0–1) compared with poor responders (96 mL/min/100 g ± 33 for ypT2–4, $P = .01$) (Table 3). Two participants did not undergo surgery for personal reasons and lacked the surgical specimens for evaluation; therefore, they were excluded from this particular analysis. When stratifying the study sample based on sex (Fig 5), the differences in tumor BF were driven by the male population (BF = 116 mL/min/100 g ± 20 for ypT0–1 compared with BF = 80 mL/min/100 g ± 28 for ypT2–4, $P = .006$) and were not significant for women (BF = 134 mL/min/100 g ± 23 for ypT0–1 vs BF = 122 mL/min/100 g ± 23 for ypT2–4, $P = .59$). No other parameters from the functional MRI were associated with response to the neoadjuvant treatment. No circulating factors were associated with ypT (Table E5 [online]).

Survival

Low tumor BF was associated with shorter PFS (hazard ratio [HR] = 0.97; 95% confidence interval: 0.96, 0.98; $P < .001$) for stage 1–3 tumors and shorter OS for the whole study sample (HR = 0.98; 95% confidence interval: 0.97, 0.99; $P < .001$) (Table 4; Fig 6a, 6b). Figures E2–E4 (online) show representative T2-weighted images with tumor BF as an overlay. Furthermore, in participants undergoing neoadjuvant treatment, low tumor BF was also associated with shorter OS (Table 4). Low D^*, which has been previously shown to be correlated with tumor BF (10), was also associated with shorter PFS (HR = 0.82; 95% confidence interval: 0.70, 0.96; $P = .01$) (Table 4, Fig 6c). No other functional MRI parameters were associated with PFS (for example, K^{trans}: HR = 0.01, $P = .25$; ΔR_2^*-peak: HR = 0.97, $P = .57$; f: HR = 0.04, $P = .40$) or OS (see Table E6 [online] for full list of results). Sex, which was associated with BF, was not a prognostic factor of PFS (HR = 1.4; 95% confidence interval: 0.5, 3.7; $P = .54$) or OS (HR = 1.2; 95% confidence interval: 0.5, 2.7; $P = .63$), with female as reference. BF remained a significant parameter in the multivariable analysis (HR = 0.97; 95% confidence interval: 0.96, 0.99; $P < .001$) (Table 4).

Discussion

To investigate individual patients' biologic tumor features related to treatment outcome, we explored predictive and prognostic values of functional MRI parameters of tumor perfusion as a surrogate measure of hypoxia. Low tumor blood flow (BF) from dynamic susceptibility contrast MRI was a prognostic marker of both adverse progression-free survival (PFS) (hazard ratio [HR] = 0.97, $P < .001$) and overall survival (HR = 0.98, $P < .001$) and was predictive of poor tumor response to neoadjuvant treatment (120 mL/min/100 g ± 21 for ypT0–1 vs 96 mL/min/100 g ± 33 for ypT2–4). Area under the curve $(AUC)_{30}$ was higher in participants without lymph node involvement compared with those with lymph node involvement (0.19 ± 0.12 vs 0.09 ± 0.03, $P = .001$). D^* from intravoxel incoherent motion MRI was associated with tumor BF and PFS (HR = 0.82, $P = .01$). Sex differences were revealed, with men having lower BF than women at stage 4 disease (74 mL/min/100 g ± 26 vs 125 mL/min/100 g ± 27, $P < .001$). MRI findings were supported by higher levels of lactate dehydrogenase (264 U/L ± 114 vs 165 U/L ± 31) and carcinoembryonic antigen (38.0 μg/L ± 18.8 vs 6.3 μg/L ± 6.5) in the blood of male participants with advanced disease.

Low tumor BF could be an important characteristic of rectal cancer aggressiveness. The underlying biology might be related to hypoxia, a condition in which poorly perfused tumors receive too little oxygen and become increasingly hypoxic and consequently have a greater potential of metastasizing (15) and becoming radioresistant (5). Neoadjuvant treatment in rectal cancer has improved local recurrence rates (16), but metastatic disease remains a challenge (17). Attempts to improve survival via intensified neoadjuvant treatment is often limited by side effects (18). This calls for new strategies, intensifying only those at high risk of metastatic progression. Hence, novel quantitative MRI parameters to identify patients at high risk are warranted.

Most dynamic contrast MRI methods are based on T1-weighted DCE MRI, but results are heterogeneous (3). DCE MRI uses the T1 relaxation effect of the contrast agent, relying on its leakage into tissue, thus measuring a combination of perfusion and capillary permeability (19). DSC MRI depends on the bolus' long-range susceptibility effect, wherein leakage has a more confounding effect because standard kinetic models assume intravascular contrast agent distribution. BF from DSC

Table 4: Uni- and Multivariable Cox Regression Analysis Predicting Shorter PFS and Shorter OS

	PFS (Stage 1–3) (n = 71)*		OS (All Participants) (n = 94)†		OS (Participants with Neoadjuvant Treatment) (n = 45)‡	
Analysis	Hazard Ratio	*P* Value	Hazard Ratio	*P* Value	Hazard Ratio	*P* Value
Univariable						
BF (mL/min/100 g)	0.97 (0.96, 0.98)	<.001§	0.98 (0.97, 0.99)	<.001§	0.98 (0.96, 0.99)	.03§
D^* (10^{-3} mm^2/s)	0.82 (0.70, 0.96)	.01§	0.9 (0.8, 1.0)	.19	0.9 (0.7, 1.1)	.16
Sex (female as reference)	1.4 (0.5, 3.7)	.54	1.2 (0.5, 2.7)	.63	1.4 (0.4, 4.3)	.61
Stage						
1 and 2‖	…		…		…	
3	2.06 (0.9, 5.0)	.11	1.5 (0.5, 4.4)	.43	4.7 (0.6, 38.0)	.15
4	NA	...	6.5 (2.5, 17.3)	<.001§	12 (1, 100)	.02§
ypT (0–1 vs 2–4)	NA#	...	NA#	...	3.7 (0.5, 28)	.21
ypN (0 vs 1–2)	NA#	...	NA#	...	2.4 (0.7, 7.9)	.14
Multivariable						
BF (mL/min/100 g)	0.97 (0.96, 0.99)	<.001§	0.98 (0.97, 0.99)	.001§	0.98 (0.96, 0.99)	.01§
Stage						
1 and 2§	…	.28	…	.73	…	.15
3	1.6 (0.7, 4.0)	...	1.2 (0.4, 3.5)	<.001§	5 (0.6, 38.4)	.01§
4	NA**	...	6 (2, 16)	...	15 (2, 133)	...

Note.—The results for progression-free survival (PFS) include participants with stage 1–3 cancer, as those with metastasis at the time of diagnosis were excluded. Cox regression analysis was performed with blood flow (BF) and pseudodiffusion coefficient (D^*) as continuous variables, whereas other variables (sex and disease stage) were categorical. Median follow-up for participants was 41 months (range, 25–71 months). Data in parentheses are the 95% confidence interval. NA = not applicable, OS = overall survival, ypT/ypN = pathologically determined T/*N*-stage after neoadjuvant treatment.

* 23 events, 48 censored.

† 32 events, 62 censored.

‡ 15 events, 30 censored.

§ *P* value indicates a significant difference.

‖ Stage 1 and 2 as reference.

Not applicable for patients without neoadjuvant treatment.

** Stage 4 participants are not included in the PFS analysis.

MRI more directly estimates perfusion; thus, high BF reflects good blood supply to the tumor.

Sex differences in tumor BF were not explained by tumor size or location, but they might relate to hormonal influence in progression of rectal tumors, linked to the angiogenic process. The role of female sex hormones in colorectal cancer has been demonstrated by Norwegian (20) and Danish (21) studies, where hormone therapy for postmenopausal women lowered risk of advanced colorectal cancers. The idea that men are more prone to having hypoxic tumors at higher stages was supported by higher levels of lactate dehydrogenase and carcinoembryonic antigen, serologic factors associated with tumor hypoxia (22,23). Furthermore, women with lower tumor stages had higher vascular endothelial growth factor A, which may indicate that in women, early stage rectal cancer recruits more blood vessels. This may not be surprising, as female sex hormones are linked to angiogenesis (24) and vascular endothelial growth factor A activation (25).

The association between D^* and PFS was less discriminating than for BF, but D^* was obtained without a contrast agent. DW MRI is suitable for patients with contraindications to gadolinium-based contrast agents and is less resource intensive and may therefore be an alternative to contrast agent–based imaging.

Several MRI parameters, all associated with tumor vascularity, were predictive of lymph node dissemination, supporting the theory that the tumor microenvironment is decisive in the early metastatic process. Tumor BF did not significantly predict pN stage, which suggests that MRI parameters related to pN reflect other hemodynamic tumor features, possibly linked to the leakiness of the vasculature.

Our study had limitations. It was a single-center study, scanning on one system only. We did not perform leakage correction of DSC MRI, as leakage correction methods are developed for use in the brain and rely on identifying nonleaky reference tissue (26). These methods only correct the blood volume estimate, which we did not attempt to estimate. However, simpler kinetic modeling makes DSC MRI more robust and more clinically relevant than DCE MRI. It is convenient to use DSC MRI to determine cancer aggressiveness because MRI is already part of standard clinical work-up, and the sequence only tracks the first pass of the bolus and is therefore not time consuming. Our multiecho MRI resulted in several excluded participants, and

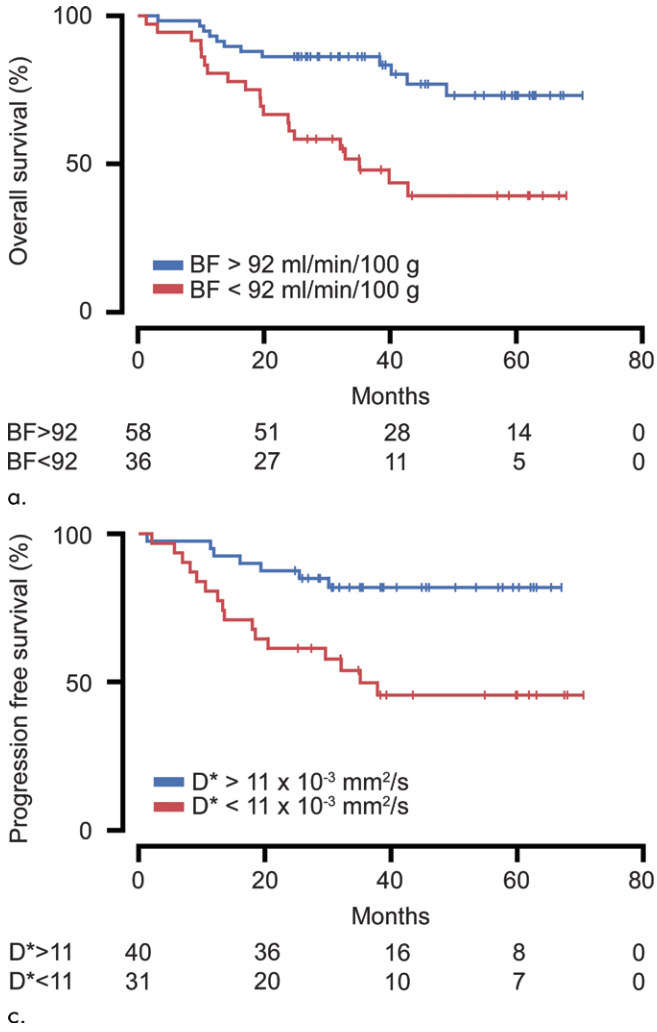

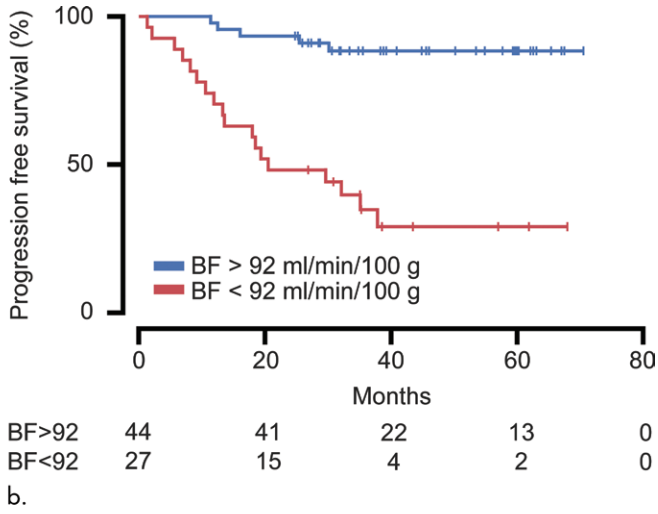

Figure 6: **(a)** Overall survival for all participants ($n = 94$), **(b)** progression-free survival for participants with stage 1–3 cancer ($n = 71$) stratified in groups of high and low blood flow (BF), and **(c)** progression-free survival for participants with stage 1–3 cancer ($n = 71$), stratified in groups of high and low pseudodiffusion D^*. Patients were categorized based on optimal cutoffs from receiver operating characteristics curves.

further protocol optimization might be necessary before clinical implementation. Other limitations include lack of study-specific posttreatment MRI and multiple comparison correction. Our results are preliminary in nature, and our findings will require further validation in larger and external cohorts.

In conclusion, tumor blood flow from dynamic susceptibility contrast MRI was found to be a prognostic marker of both progression-free survival and overall survival as well as predictive of local tumor response to neoadjuvant treatment in rectal cancer. We revealed sex differences in tumor perfusion and disease progression, which is interesting for future research to dissect the role of underlying tumor biology.

Author contributions: Guarantors of integrity of entire study, K.M.B., K.R.R.; study concepts/study design or data acquisition or data analysis/interpretation, all authors; manuscript drafting or manuscript revision for important intellectual content, all authors; approval of final version of submitted manuscript, all authors; agrees to ensure any questions related to the work are appropriately resolved, all authors; literature research, K.M.B., S.M., K.R.R.; clinical studies, K.M.B., E.G., A.N., S.H.H., K.I.G., A.B., A.H.R., K.R.R.; statistical analysis, K.M.B., S.M.; and manuscript editing, K.M.B., S.M., E.G., A.N., S.H.H., A.H.R., K.R.R.

Disclosures of Conflicts of Interest: **K.M.B.** disclosed no relevant relationships. **S.M.** Activities related to the present article: disclosed no relevant relationships. Activities not related to the present article: institution received funding from the Kolbjørn Brambani research foundation and Blix Family Research Foundation. Other relationships: disclosed no relevant relationships. **E.G.** disclosed no relevant relationships. **A.N.** disclosed no relevant relationships. **S.H.H.** disclosed no relevant relationships. **K.I.G.** disclosed no relevant relationships. **A.B.** Activities related to the present article: disclosed no relevant relationships. Activities not related to the present article: is a consultant for, receives royalties from, and holds stock in NordicNeuroLab. Other relationships: disclosed no relevant relationships. **A.H.R.** disclosed no relevant relationships. **K.R.R.** Activities related to the present article: disclosed no relevant relationships. Activities not related to the present article: has a patent with and receives royalties from NordicICE. Other relationships: disclosed no relevant relationships.

References

1. Bray F, Ferlay J, Soerjomataram I, Siegel RL, Torre LA, Jemal A. Global cancer statistics 2018: GLOBOCAN estimates of incidence and mortality worldwide for 36 cancers in 185 countries. CA Cancer J Clin 2018;68(6):394–424.
2. Larsen IK, Møller B, Johannesen TB, et al. Cancer in Norway 2017 - Cancer incidence, mortality, survival and prevalence in Norway. Oslo, Norway: Cancer Registry of Norway, 2018.
3. Dijkhoff RAP, Beets-Tan RGH, Lambregts DMJ, Beets GL, Maas M. Value of DCE-MRI for staging and response evaluation in rectal cancer: a systematic review. Eur J Radiol 2017;95:155–168.
4. Le Bihan D, Breton E, Lallemand D, Aubin ML, Vignaud J, Laval-Jeantet M. Separation of diffusion and perfusion in intravoxel incoherent motion MR imaging. Radiology 1988;168(2):497–505.
5. Horsman MR, Overgaard J. The impact of hypoxia and its modification of the outcome of radiotherapy. J Radiat Res (Tokyo) 2016;57(suppl 1):i90–i98.
6. Rankin EB, Giaccia AJ. Hypoxic control of metastasis. Science 2016;352(6282):175–180.
7. Glimelius B, Tiret E, Cervantes A, Arnold D; ESMO Guidelines Working Group. Rectal cancer: ESMO Clinical Practice Guidelines for diagnosis, treatment and follow-up. Ann Oncol 2013;24(Suppl 6):vi81–vi88.
8. Glynne-Jones R, Wyrwicz L, Tiret E, et al. Rectal cancer: ESMO Clinical Practice Guidelines for diagnosis, treatment and follow-up. Ann Oncol 2017;28(suppl 4):iv22–iv40 [Published correction appears in Ann Oncol 2018;29(suppl 4):iv263.].
9. Grøvik E, Redalen KR, Storås TH, et al. Dynamic multi-echo DCE- and DSC-MRI in rectal cancer: low primary tumor K^{trans} and $\Delta R2^*$ peak are significantly associated with lymph node metastasis. J Magn Reson Imaging 2017;46(1):194–206.
10. Bakke KM, Grøvik E, Meltzer S, et al. Comparison of intravoxel incoherent motion imaging and multiecho dynamic contrast-based MRI in rectal cancer. J Magn Reson Imaging 2019;50(4):1114–1124.
11. Grøvik E, Bjørnerud A, Storås TH, Gjesdal K-I. Split dynamic MRI: single bolus high spatial-temporal resolution and multi contrast evaluation of breast lesions. J Magn Reson Imaging 2014;39(3):673–682.
12. Tofts PS. Modeling tracer kinetics in dynamic Gd-DTPA MR imaging. J Magn Reson Imaging 1997;7(1):91–101.

13. Østergaard L, Weisskoff RM, Chesler DA, Gyldensted C, Rosen BR. High resolution measurement of cerebral blood flow using intravascular tracer bolus passages. Part I: Mathematical approach and statistical analysis. Magn Reson Med 1996;36(5):715–725.
14. Heidari S, Babor TF, De Castro P, Tort S, Curno M. Sex and Gender Equity in Research: rationale for the SAGER guidelines and recommended use. Res Integr Peer Rev 2016;1(1):2.
15. Gilkes DM, Semenza GL, Wirtz D. Hypoxia and the extracellular matrix: drivers of tumour metastasis. Nat Rev Cancer 2014;14(6):430–439.
16. Aklilu M, Eng C. The current landscape of locally advanced rectal cancer. Nat Rev Clin Oncol 2011;8(11):649–659.
17. Bosset JF, Calais G, Mineur L, et al. Fluorouracil-based adjuvant chemotherapy after preoperative chemoradiotherapy in rectal cancer: long-term results of the EORTC 22921 randomised study. Lancet Oncol 2014;15(2):184–190.
18. Ree AH, Meltzer S, Flatmark K, Dueland S, Kalanxhi E. Biomarkers of treatment toxicity in combined-modality cancer therapies with radiation and systemic drugs: study design, multiplex methods, molecular networks. Int J Mol Sci 2014;15(12):22835–22856.
19. Sourbron SP, Buckley DL. On the scope and interpretation of the Tofts models for DCE-MRI. Magn Reson Med 2011;66(3):735–745.
20. Botteri E, Støer NC, Sakshaug S, et al. Menopausal hormone therapy and colorectal cancer: a linkage between nationwide registries in Norway. BMJ Open 2017;7(11):e017639.
21. Mørch LS, Lidegaard Ø, Keiding N, Løkkegaard E, Kjær SK. The influence of hormone therapies on colon and rectal cancer. Eur J Epidemiol 2016;31(5):481–489.
22. Serganova I, Rizwan A, Ni X, et al. Metabolic imaging: a link between lactate dehydrogenase A, lactate, and tumor phenotype. Clin Cancer Res 2011;17(19):6250–6261.
23. Kokkonen N, Ulibarri IF, Kauppila A, et al. Hypoxia upregulates carcinoembryonic antigen expression in cancer cells. Int J Cancer 2007;121(11):2443–2450.
24. Trenti A, Tedesco S, Boscaro C, Trevisi L, Bolego C, Cignarella A. Estrogen, angiogenesis, immunity and cell metabolism: solving the puzzle. Int J Mol Sci 2018;19(3):E859.
25. Caliceti C, Aquila G, Pannella M, et al. 17β-estradiol enhances signalling mediated by VEGF-A-delta-like ligand 4-notch1 axis in human endothelial cells. PLoS One 2013;8(8):e71440.
26. Bjørnerud A, Sorensen AG, Mouridsen K, Emblem KE. T1- and T2*-dominant extravasation correction in DSC-MRI: part I--theoretical considerations and implications for assessment of tumor hemodynamic properties. J Cereb Blood Flow Metab 2011;31(10):2041–2053.